Electronic-Structure-Dependent Bacterial Cytotoxicity of Single-Walled Carbon Nanotubes

Chad D. Vecitis,[†,*] Katherine R. Zodrow, Seoktae Kang, and Menachem Elimelech

Department of Chemical and Environmental Engineering, Yale University, New Haven, Connecticut 06520-8286. [†]Current address: School of Engineering and Applied Sciences, Harvard University, Cambridge, Massachusetts 02144.

ABSTRACT Single-walled carbon nanotubes (SWNTs) have been previously observed to be strong antimicrobial agents, and SWNT coatings can significantly reduce biofilm formation. However, the SWNT antimicrobial mechanism is not fully understood. Previous studies on SWNT cytotoxicity have concluded that membrane stress (*i.e.*, direct SWNT—bacteria contact resulting in membrane perturbation and the release of intracellular contents) was the primary cause of cell death. Gene expression studies have indicated oxidative stress may be active, as well. Here, it is demonstrated for the first time how SWNT electronic structure (*i.e.*, metallic *versus* semiconducting) is a key factor regulating SWNT antimicrobial activity. Experiments were performed with well-characterized SWNTs of similar length and diameter but varying fraction of metallic nanotubes. Loss of *Escherichia coli* viability was observed to increase with an increasing fraction of metallic SWNTs. Time-dependent cytotoxicity measurements indicated that in all cases the majority of the SWNT antimicrobial action occurs shortly after (<15 min) bacteria—SWNT contact. The SWNT toxicity mechanism was investigated by *in vitro* SWNT-mediated oxidation of glutathione, a common intracellular thiol that serves as an antioxidant and redox state mediator. The extent of glutathione oxidation was observed to increase with increasing fraction of metallic SWNTs, indicating an elevated role of oxidative stress. Scanning electron microscopy images of *E. coli* in contact with the SWNTs demonstrated electronic structure-dependent morphological changes consistent with cytotoxicity and glutathione oxidation results. A three-step SWNT antimicrobial mechanism is proposed involving (i) initial SWNT—bacteria contact, (ii) perturbation of the cell membrane, and (iii) electronic structure-dependent bacterial oxidation.

KEYWORDS: carbon nanotube · bacterial cytotoxicity · oxidative and membrane stress · SWNT electronic structure · glutathione

Nanotechnology involves the application of nano- or quantum-sized materials that possess unique properties as compared to bulk materials of similar composition. Carbon-based nanomaterials such as fullerenes[1] and carbon nanotubes (CNTs)[2,3] are of particular interest due to their strong mechanical and tunable electronic properties, resulting in a wide range of technological applications.[4] Consequently, CNT production is growing exponentially and is an emerging multibillion dollar per year market.[5,6] Environmental carbon-based nanotechnology is a promising area of growth due to potential applications in the fields of sensors, water treatment, and alternative energy.[7] However, the environmental implications of CNTs in terms of dispersion, fate, and ecotoxicological and human health impacts should be better understood prior to their widespread application.[8]

Recent studies have reported that most carbon-based nanomaterials are cytotoxic to bacteria,[9−11] with single-walled carbon nanotubes (SWNTs) exhibiting the strongest antimicrobial activity.[12−15] SWNT bacterial cytoxicity has environmental implications regarding the impact of SWNT micropollutants on aquatic ecosystems. Results of a recent study[16] indicate biofilm formation is also significantly reduced by SWNT surface coatings. The effectiveness of SWNTs as antimicrobial agents is attributed to their unique physicochemical properties such as small diameter (<5 nm) and high aspect ratio. However, the SWNT antimicrobial mechanism is not completely understood.

Previous studies reported physical membrane perturbation as the most likely SWNT cytotoxicity mechanism.[12−15] A recent CNT toxicity study utilizing gene expression indicated that an oxidative stress mechanism may also play a role.[17] The mechanism may be the simultaneous or sequential combination of membrane stress and oxidative stress, possibly acting synergistically. Determining the true mechanism, however, is not trivial. For example, initial studies suggested that *n*C60 cytotoxicity was likely due to reactive oxygen species (ROS) production.[18,19] However, later studies determined that the *n*C60−dye interactions were responsible for the positive ROS results,[20] and that ROS-independent oxidation of membrane proteins and lipids was the more likely mechanism.[10,11]

Previously, insight on the SWNT bacterial cytotoxicity mechanism resulted from the relative toxicity as a function of CNT

*Address correspondence to vecitis@seas.harvard.edu.

Received for review July 7, 2010 and accepted August 25, 2010.

Published online September 2, 2010. 10.1021/nn101558x

physicochemical properties, including diameter,[17] surface functionality,[14,21] and dispersion/aggregation state.[9,13] One important SWNT physicochemical property affecting reactivity that has not been investigated in terms of cytotoxicity is electronic structure (*i.e.*, metallic *versus* semiconducting). There are an infinite number of carbon nanotube atomic structures, which are defined by the helical arrangement of the carbon atoms and diameter of the nanotubes. Statistically, one-third of these structures are pseudometallic and the other two-thirds are semiconducting.[22,23] Investigations into SWNT electronic structure-dependent cytotoxicity are hindered by the lack of synthetic methods that can produce a single SWNT atomic structure.[24,25] However, recent advances in ultracentrifugation-based SWNT purification have resulted in a technology that can sort a heterogeneous mixture of SWNTs by diameter, band gap, or electronic structure,[26] thereby allowing for SWNT electronic structure-dependent bacterial cytotoxicity to be evaluated.

The electronic structure-dependent chemical reactivity of SWNTs has been documented. Metallic SWNTs were observed to be significantly more reactive than semiconducting SWNTs of similar diameter.[27−31] For example, diazonium species,[27] OsO_4,[28] NO_2^+ formed in HNO_3/H_2SO_4 mixtures,[29] methane plasmas,[30] and perfluorinated olefins[31] were observed to react with metallic SWNTs at significantly faster rates than semiconducting SWNTs of a similar diameter. The faster metallic SWNT reaction rates were due to a greater conductivity and electron density near the SWNT Fermi level. It is, therefore, plausible to hypothesize that the increased metallic SWNT chemical reaction kinetics may also affect their bacterial cytotoxicity.

Here, how the electronic structure of SWNTs affects their antimicrobial activity toward the Gram-negative bacteria, *Escherichia coli*, is investigated. Specifically, the cytotoxicity of three purified and well-characterized SWNTs of similar diameter and length, but varying fraction (<5, ~30, >95%) of metallic SWNTs is evaluated. A SWNT bacterial-cytotoxicity mechanism is proposed to explain the experimental results.

RESULTS AND DISCUSSION

The high (>95%) and low (<5%) percentage metallic (M) SWNT samples used in this study were separated by density gradient ultracentrifugation using a sodium dodecyl sulfate/sodium cholate cosurfactant system (NanoIntegris).[26] Key physicochemical properties of the three SWNT samples—semiconducting ("S", <5% M), mixed ("X", ~30% M), and metallic ("M", >95% M)—are summarized in Table 1. The surfactant-dispersed metallic (green-blue) and semiconducting (brown) tubes can be visually identified (Figure 1A), and the UV−vis spectra (Figure 1C) have characteristic adsorption peaks in the M_{11} (600−800 nm) and S_{22} (900−1100 nm) regions, respectively. The absorption peaks roughly correspond

TABLE 1. Physicochemical Properties of SWNTs Evaluated for *E. coli* Cytotoxicity

	diameter (nm)[a]	length (μm)[b]	G/D[c]	electronic
SWNT-S	1.4 ± 0.3	1−4	2.7	<5% metallic
SWNT-X	1.4 ± 0.3	1−4	2.1	~30% metallic
SWNT-M	1.4 ± 0.3	1−3	2.1	>95% metallic

[a]The diameters of the SWNTs are determined separately by TEM, vis−NIR, Raman. [b]Lengths are of primary SWNT bundles from TEM. [c]G/D ratios are determined from 785 nm excitation Raman spectra.

to SWNT diameters for both metallic and semiconducting tubes of 1.4 nm.[32] SWNTs were precipitated from the surfactant solution, collected by filtration, and washed with copious amounts of water, as recommended by the manufacturer. The filtered SWNTs were bath sonicated in concentrated HCl to remove metal catalyst impurities without oxidizing the nanotube walls.[33] The SWNTs were then heated to 350 °C for 6 h to remove residual amorphous carbon. Representative TEM images (Figure 1B,D and Figure S3) indicated negligible SWNT impurities, consistent with SEM images (Figure S2). TEM image analysis (ImageJ, NIH) yielded semiconducting SWNT lengths of 1−4 μm, metallic SWNT lengths of 1−3 μm, and SWNT diameters of 1.4 ± 0.3 nm, in agreement with diameter estimations from UV−vis data. Raman spectra measured using 785 nm excitation (Figure S1) were used to calculate G-band to D-band ratios (G/D) of >2 for all SWNTs, indicating the nanotubes were relatively free of defects and impurities, as also observed by TEM. Raman RBM peak analysis indicated the median diameter of the metallic tubes to be 1.42 nm and the semiconducting tubes to be 1.36 nm, in agreement with the UV−vis and TEM diameter calculations.

Escherichia coli K12 was used to evaluate the SWNT toxicity. Bacteria were grown in Luria−Bertani (LB) broth and washed twice with isotonic saline (0.9 w/v % NaCl) solution to eliminate effects of cell culture media constituents on SWNT cytotoxicity. SWNT toxicity toward *E. coli* was evaluated both with suspended cells and cells deposited on an SWNT-coated filter—two methods that have been previously observed to yield similar results.[12,17] For experiments using suspended cells, SWNTs (1 μg/mL) and *E. coli* (10^7 cells/mL) were incubated in saline solution for 1 h at 37 °C. For the filter experiments, a SWNT-coated filter was prepared (Millipore, 5 μm, PTFE, 35 mm in filterable diameter) and ~10^6 cells were gently deposited on the SWNTs by vacuum filtration. The SWNT-induced viability loss was determined by fluorescence microscopy as previously described.[12] Briefly, 4′,6-diamidino-2-phenylindole (DAPI, membrane permeable dye) was used to stain all cells, and propidium iodide (PI, membrane impermeable dye) was used to stain membrane perturbed cells with reduced viability. Approximately 200−300 total cells were counted per image, and the viability loss was taken as the average of 8−10 images. The bacterial vi-

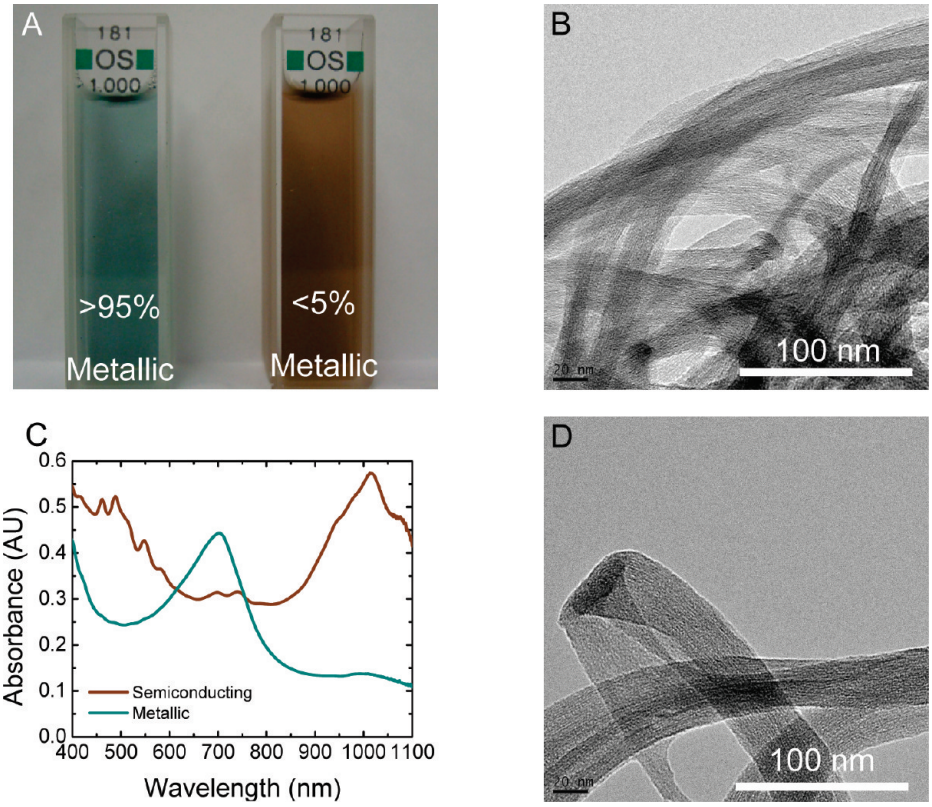

Figure 1. SWNT characterization. (A) Vis−NIR samples of 100 μg/mL surfactant-dispersed SWNTs; metallic (left), semiconducting (right). (B) TEM of metallic SWNTs. (C) Vis−NIR spectra of metallic (blue) and semiconducting (brown) SWNTs. (D) TEM of semiconducting SWNTs.

ability loss was calculated as the PI stained cells divided by the total (DAPI and PI) stained cells. For experiments using suspended cells, only cells adhered to the SWNT aggregates were quantified.

Representative fluorescence microscope images of the semiconducting (<5% M) and the metallic (>95% M) SWNT suspended toxicity assay are presented in Figure 2A,C and Figure 2B,D, respectively. Large SWNT−bacteria aggregates (>100 μm) formed during incubation in the isotonic saline solution. The bacterial density is significantly greater on the surface of the aggregates as compared to in solution, indicating the *E.*

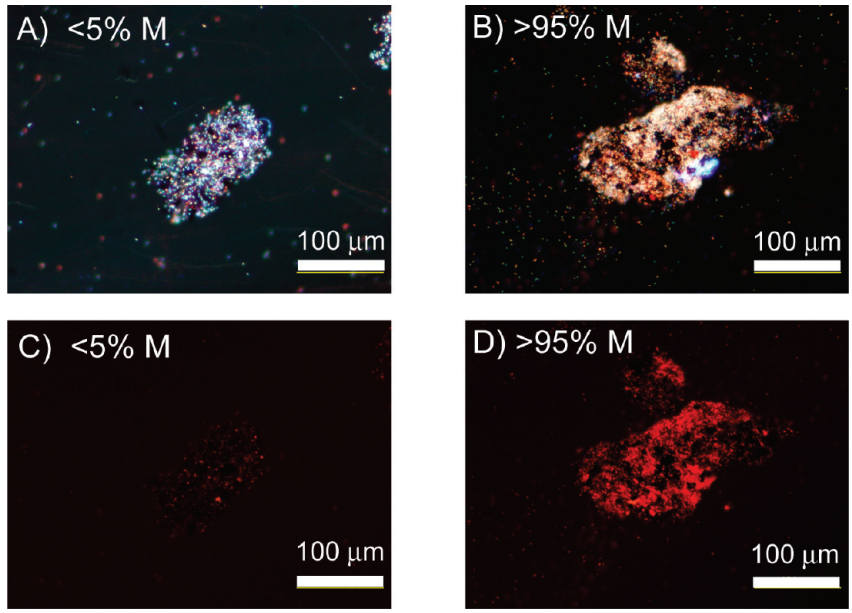

Figure 2. Fluorescent staining of *E. coli*−SWNT aggregates. (A) DAPI (blue, viable) and PI (red, nonviable) staining of bacteria with <5% metallic SWNTs. (B) DAPI and PI staining of bacteria with >95% metallic SWNTs. (C) PI staining of bacteria and <5% metallic SWNTs. (D) PI staining of bacteria and >95% metallic SWNTs.

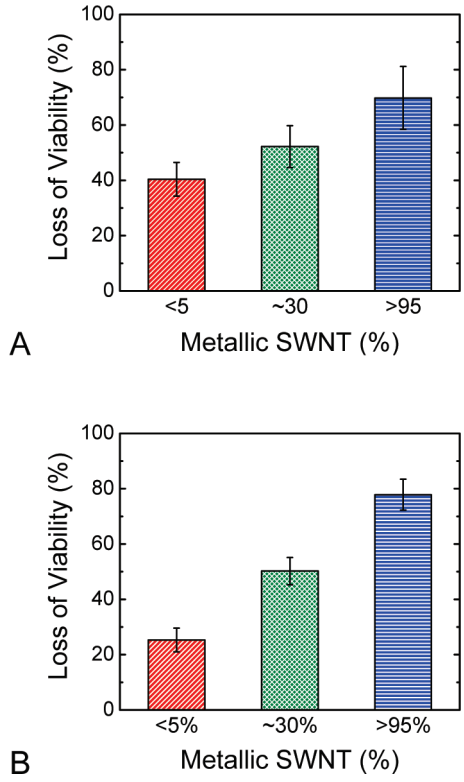

Figure 3. Loss of *E. coli* viability *versus* percent metallic SWNTs. Semiconducting (<5% M, red), mixed (~30% M, green), and metallic (>95% M, blue) during (A) the aggregate assay experiment and (B) the deposition assay experiment.

coli preferentially attached to the surface of the SWNTs. Visual inspection of the combined DAPI and PI fluorescence images revealed that the bacteria interacting with the metallic SWNTs (Figure 2B, predominantly red) had a significantly greater loss of viability than the bacteria interacting with the semiconducting SWNTs (Figure 2A, predominantly blue). This was confirmed by inspection of the PI-only fluorescence images as most of the bacteria attached to the metallic tubes (Figure 2D) were stained with PI and only a few bacteria attached to the semiconducting tubes (Figure 2C) were stained with PI.

The results of this qualitative visual inspection were confirmed by the quantitative live−dead analysis from the aggregate and filter toxicity assay, as shown in Figure 3A,B, respectively. Notably, the percent loss of viability of *E. coli* attached to the SWNT filter was correlated to the fraction of metallic (M) SWNTs in both the aggregate (40 ± 6%, <5% M; 52 ± 8%, ~30% M; 70 ± 11%, >95% M) and filter (25 ± 4%, <5% M; 50 ± 5%, ~30% M; 78 ± 6%, >95% M) toxicity assays. Our results demonstrated for the first time that SWNT toxicity is correlated to its electronic structure in bacteria. The greater toxicity of the metallic nanotubes indicated that, after SWNT−bacteria contact and physical perturbation of the cell membrane, the metallic tubes may induce oxidative stress that is not present with semiconducting SWNTs. There are a number of possible SWNT−bacteria oxidative stress pathways. For example, similar to the antimicrobial mechanism reported for *n*C60,[10,11] the metallic SWNTs may directly oxidize the bacteria *via* a process similar to Fermi level equilibration.[34,35] Alternatively, due to the micrometer length and conductive properties, metallic SWNTs could "short-circuit" the bacteria by acting as a conductive bridge over the insulating lipid bilayer, releasing cellular energy into the external environment.

In both the suspended and deposited assays, the loss of *E. coli* viability was correlated to the percent of metallic SWNTs. However, the toxicity of the metallic sample was reduced (78 to 70%), the toxicity of the mixed sample remains unchanged (50 to 52%), and the toxicity of the semiconducting sample was increased (25 to 40%) in the aggregate assay (Figure 3A) as compared to the filter assay (Figure 3B). A primary difference between the two assays was the aggregate state of the SWNTs since the suspended experiments were completed in 0.9% NaCl, resulting in large SWNT aggregate structures, whereas the SWNT filters were prepared with freshly sonicated, well-dispersed SWNTs in DMSO (rinsed with ethanol and water to remove residual DMSO). Thus, the variance between the suspended and deposited toxicity experiments was likely due to the SWNTs being significantly more aggregated during the suspended experiments. CNT cytotoxicity has been previously reported to be correlated to aggregation state. Kang *et al.*[21] observed that *E. coli* toxicity of MWNT deposit layers increased with increasing aqueous dispersivity of MWNTs and suggested this was due to an increase in the effective nanotube surface area in contact with bacterial cells. Liu *et al.*[13] observed that surfactant-dispersed SWNTs were significantly more toxic than highly aggregated SWNTs in isotonic saline. The decrease in the toxicity of the >95% metallic SWNTs in going from the filter assay to the suspended assay is consistent with the previous studies discussed above. In contrast, the semiconducting (<5% M) SWNTs displayed a contradictory trend, with toxicity increasing from the filter assay to the suspended assay. This contradictory result suggests that the suspended aggregate structure of the semiconducting SWNT sample may have more effective surface area than the DMSO filtered SWNT mat. It also suggests that the aqueous SWNT aggregate structure is a function of the fraction metallic tubes; however, further in-depth investigations will be required to understand any electronic-structure-dependent aggregation.

The loss of viability as a function of time for the three SWNT samples is plotted in Figure 4A. The *E. coli* viability loss reached a maximum after 15 min of contact with the semiconducting SWNTs and after 25 min of contact with the mixed and metallic SWNTs. The viability loss increased another 15−20% between the 15- and 25- min time points for the mixed and metallic SWNTs. The continued increase in toxicity with time

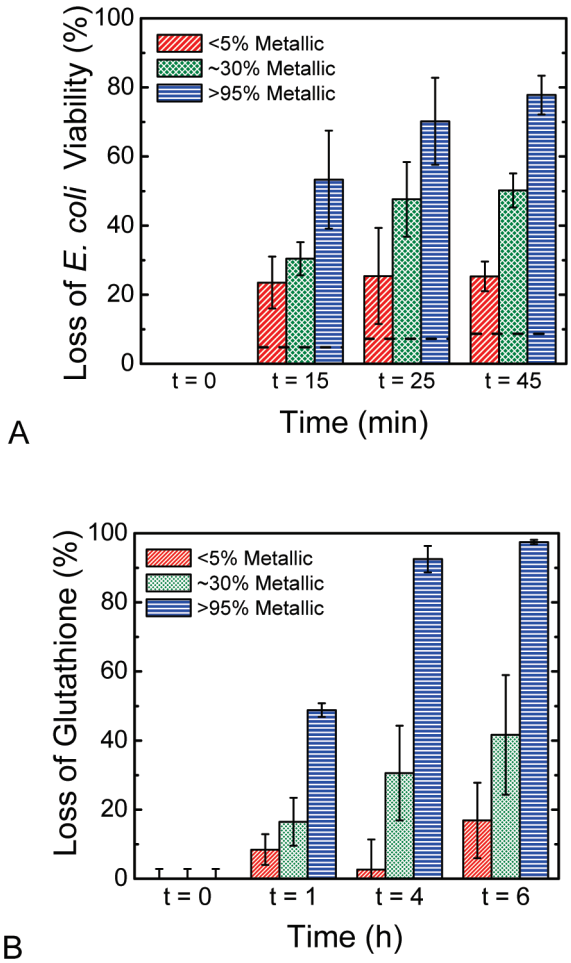

Figure 4. Loss of *E. coli* viability and *in vitro* loss of glutathione *versus* time upon exposure to SWNTs of various fraction metallic tubes. (A) Loss of SWNT filter deposited *E. coli* viability *versus* time (0 to 45 min) and fraction metallic SWNT (<5% M, red; ~30% M, green; >95% M, blue). Dashed line through data represents negative control of *E. coli* on PTFE filter with no SWNTs. (B) *In vitro* loss of glutathione *versus* time (0 to 6 h) and fraction metallic SWNT (<5% M, red; ~30% M, green; >95% M, blue; $[GSH]_i$ = 0.4 mM; pH 8.6).

for the greater fraction metallic SWNTs suggests that the metallic-specific antimicrobial activity (electronic structure-based oxidative stress) may occur shortly after the nonspecific SWNT antimicrobial activity (membrane stress) observed for the semiconducting SWNTs. This is a logical conclusion considering that intimate contact between the bacteria and the SWNTs is necessary for SWNT-mediated electron transfer. It is of note that in all cases, the majority of the antimicrobial action occurs in less than 15 min, shortly after SWNT−bacteria contact.

The mechanism of increasing loss of *E. coli* viability with increasing fraction metallic SWNT is hypothesized to be due to the metallic SWNT-mediated cellular oxidative stress. For example, glutathione (GSH), a small, three-residue thiol-containing polypeptide, is present at high levels (1−10 mM) in most Gram-negative bacteria.[36] Glutathione aids in maintenance of the cell redox environment and has been suggested to regulate the biological status of eukaryotic cells (*e.g.*, proliferation, differentiation, apoptosis) since significant GSH oxidation into its disulfide (GSSG) is correlated with cell death.[37] GSH is also known to protect against oxidative stress.[38,39] Intracellularly, GSH is predominantly found in its reduced form but will spontaneously oxidize upon exposure to the extracellular molecular oxygen (O_2 + 2R-SH → RSSR + H_2O_2; $\Delta G^0 = -96$ kJ/mol).[38] Thus, a conductive metallic SWNT bridge over the lipid bilayer could electronically expose GSH to external conditions, resulting in its oxidation. Therefore, *in vitro* glutathione oxidation is an indirect measure of ability to induce cellular oxidative stress.

The loss of glutathione using Ellman's assay[40] upon exposure to SWNTs was investigated under the reaction conditions: $[GSH]_i$ = 0.4 mM, 50 μg/mL SWNTs, $[NaHCO_3]$ = 50 mM, pH 8.6, and ~22−23 °C. Glutathione oxidation without SWNTs was used as a negative control, and the minimal oxidation observed was subtracted from all SWNT data (Figure 4B). Glutathione oxidation was observed to be mediated by all SWNT samples, similar to thiol oxidation mediated by other carbon-based materials such as black carbon[41] and natural organic matter.[42] In all cases, the extent of GSH oxidation increased with increasing SWNT exposure time. Notably, GSH oxidation proceeds more rapidly with increasing fraction of metallic SWNTs. After 1 h of SWNT exposure, the extent of GSH oxidation already showed significant correlation to the fraction metallic SWNTs (8.4 ± 4.5%, <5% M; 17 ± 6.9%, ~30% M; 48 ± 2.0%, >95% M). After 6 h of SWNT exposure, the extent of GSH oxidation increased in all SWNT samples (18 ± 10%, <5% M; 42 ± 18%, ~30% M; 98 ± 2%, >95% M). The results for the 6 h SWNT exposure indicate that nearly all of the GSH in the presence of the metallic (>95% M) SWNTs had been oxidized, whereas GSH oxidation in the presence of the semiconducting (<5% M) SWNTs was only slightly greater than the control. The more rapid oxidation of GSH by SWNTs of increased metallic fraction (Figure 4B) correlates with the increased toxicity of these SWNTs (Figure 4A). This observation suggests that the increased *E. coli* cytotoxicity of metallic SWNTs is due to their enhanced mediation of the oxidation of intracellular components such as thiols. The observation supports the hypothesis that, due to their micrometer length and conductive properties, metallic SWNTs act as a conductive bridge over the insulating lipid bilayer releasing cellular energy (2 GSH → GSSH + $2e^-$ + $2H^+$) into the external environment (O_2 + $2e^-$ + $2H^+$ → H_2O_2). The metallic SWNT-mediated oxidative stress was likely not observed in previous reports[12−15] that stated membrane stress as the primary mechanism due to the statistically low (~30%) percent of metallic SWNTs in as-synthesized SWNT batches.

Scanning electron microscopy (SEM) images of cells in contact with SWNTs revealed electronic-structure-

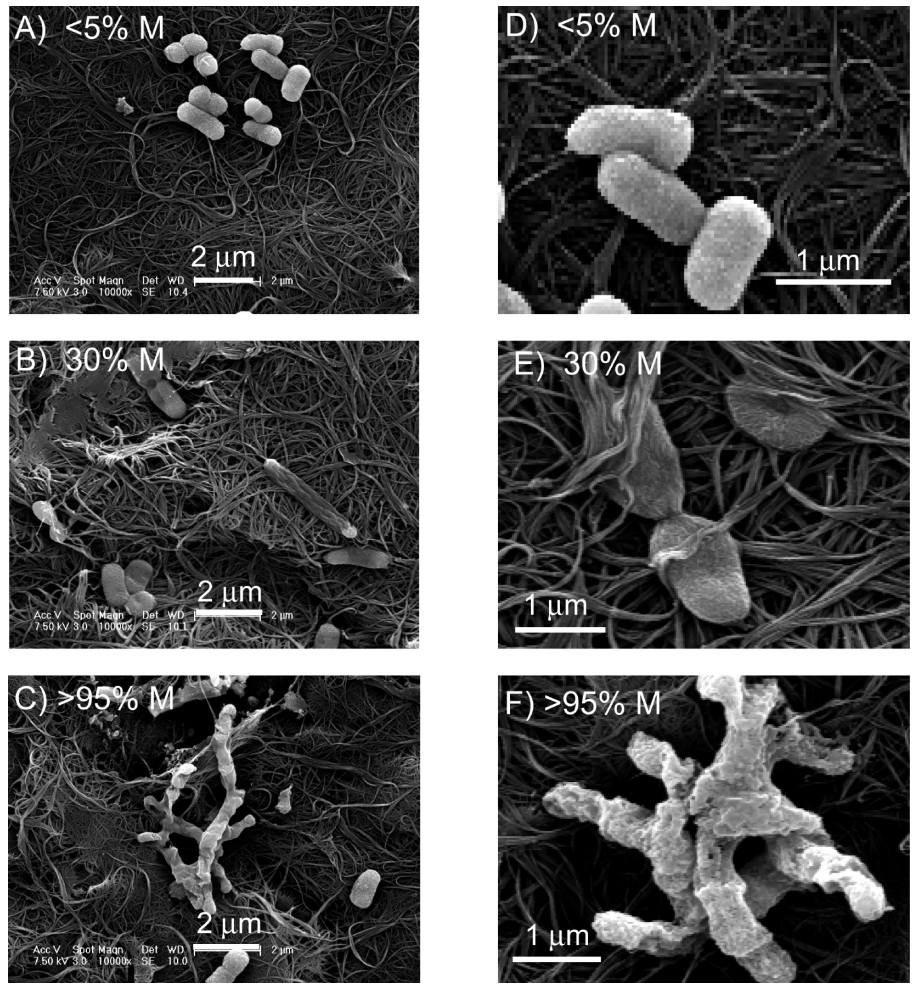

Figure 5. Representative SEM images of *E. coli* deposited on SWNT filters. *E. coli* were deposited on the SWNT filter, incubated for 45 min in isotonic saline, and fixed with glutaraldehyde and osmium tetroxide prior to SEM imaging: (A,D) <5% metallic, (B,E) 30% metallic, and (C,F) >95% metallic. Note the differences in cell membrane hydration, structure, and roughness between the three samples.

dependent morphological changes (Figure 5). After 1 h of incubation with the semiconducting (<5% M) SWNTs (Figure 5A,D), the majority of the cells were still intact and maintaining their outer membrane structure, similar to cells in the control. After 1 h of incubation with the mixed (~30% M) SWNTs (Figure 5B,E), the majority of the *E. coli* cells had lost their cellular integrity and had become elongated or flattened, indicating irreversible cell damage or cell death consistent with previous observations.[12,13,18] In contrast, the majority of the *E. coli* incubated with the metallic SWNTs (Figure 5C,F) were not only elongated and flattened, but the cell membranes also appeared to be damaged and had lost their normal structure. Moreover, the membranes of cells in contact with the metallic SWNTs had increased roughness and in some places were seemingly torn as large gaps in the membrane were observed. The extensive loss of cell membrane structure suggests that the >95% metallic SWNTs not only perturbed the cell membrane but may have also chemically degraded or oxidized the membrane. This observation is in agreement with the results from Figure 4B, indicating that metallic SWNTs can mediate the oxidation of glutathione to a significantly greater extent than semiconducting SWNTs. The images in Figure 5 demonstrate that the number of damaged cells and the extent of damage to the cells are dependent upon the SWNT electronic properties, consistent with the results in Figures 2, 3, and 4.

The results in Figures 2−5 demonstrate that the bacterial cytotoxicity of metallic SWNTs is much greater than semiconducting SWNTs and may be due to reactive SWNT−bacteria interactions resulting in oxidation of intracellular components. Here, a general SWNT toxicity mechanism is proposed that takes into account observations in this paper and previous reports on SWNT bacterial cytotoxicity. The first step is bacterial adhesion or deposition onto SWNTs resulting in direct bacteria−SWNT contact:

$$\text{Bac} + \text{SWNT} \rightarrow \text{Bac}\cdots\text{SWNT} \qquad (1)$$

As observed in Figure 2, *E. coli* density was significantly greater in the SWNT aggregates as compared to free in solution, indicating they strongly adhere to the SWNTs.

Thus, the extent of bacterial−SWNT contact will be mediated by the exposed SWNT surface area, aggregation state, and solution composition.

The subsequent mechanistic steps follow the approach previously utilized for describing the toxicity of various classes of hydrocarbons toward aquatic microorganisms.[43] The nonspecific or baseline hydrocarbon toxicity is described as its ability to disrupt the cell membrane, and the specific or "reactive" toxicity is described as how the hydrocarbon affects membrane proton transport, disrupts specific proteins, or chemically oxidizes proteins, lipids, and DNA.[44] The nonspecific toxicity is generally related to the compound's hydrophobicity (*i.e.*, tendency to partition into cell membrane causing stress), and the specific reactive toxicity is often related to the compound's "electrophilicity" (*i.e.*, tendency to oxidize cellular material causing stress).[45] Thus, step 2 in the SWNT antimicrobial mechanism involves cell membrane perturbation:

$$\text{Bac}\cdots\text{SWNT} \rightarrow (\text{Bac} < \text{SWNT}) \qquad (2)$$

where the "<" symbol indicates that the SWNT has made intimate, membrane disruptive contact with the bacteria. Step 2 has been observed to be active to various extents for all previously evaluated CNTs[12−15] as well as the ones evaluated here and is therefore appropriately labeled as nonspecific or membrane stress-related toxicity.

The third step in the SWNT antimicrobial mechanism will involve its ability to disrupt a specific microbial process *via* disturbing/oxidizing a vital cellular structure/component:

$$(\text{Bac} < \text{SWNT}) \rightarrow (\text{B/a/c} < \text{SWNT}) \qquad (3)$$

The "/" symbols indicate that the SWNT reactivity has disrupted a specific cellular process or structure, resulting in increased toxicity. The most common mechanism for step 3 is oxidation of bacterial lipids, proteins, and DNA or oxidative stress. The results presented here indicate that metallic SWNTs of similar diameter and length participate in the reactive events described by eq 3 to a much greater extent than semiconducting SWNTs. One such example of the eq 3 events proposed here for the increased toxicity of metallic SWNTs is that they act as a conductive bridge over the insulating lipid bilayer, mediating electron transfer from bacterial intracellular components to the external environment (*e.g.*, $O_2 + 2\ \text{R-SH} \rightarrow \text{RSSR} + H_2O_2$). This hypothesized mechanism is strongly supported by the observation that glutathione is more rapidly oxidized in the presence of >95% metallic SWNTs than in the presence of 30 and <5% metallic SWNTs (Figure 4B). The mechanism is also supported by SEM images of bacteria in contact with >95% metallic SWNTs (Figure 5C,F), displaying significant loss of cell membrane structure as compared to the samples containing primarily semiconducting SWNTs. If thiol oxidation is mediated by metallic SWNTs, the oxidation of the more reducing cellular energy carriers like NADH and NADPH would also occur,[37] resulting in cell death as observed here.

In conclusion, the results of this study have demonstrated for the first time that SWNT bacterial (*E. coli*) cytotoxicity is dependent on the SWNT electronic structure (*i.e.*, metallic *versus* semiconducting). Loss of *E. coli* viability was positively correlated to the fraction of metallic SWNTs in samples of similar diameter, length, and number of defect sites. The extent of glutathione oxidation also showed a positive correlation to the fraction of metallic SWNTs, indicating that the increased cytotoxicity may be due to increased cellular oxidative stress (as opposed to membrane stress cited in previous reports). This result is consistent with SEM images of *E. coli* morphological changes that showed an increase in loss of cell membrane integrity with increasing fraction of metallic SWNTs. Our results have strong implications toward evaluating the environmental impact of SWNTs on aquatic ecosystems and the importance of characterizing all SWNT physicochemical properties, including electronic structure, when completing these evaluations. Even more important are the possible applications of metallic SWNTs as antimicrobial agents, for example, as a possible replacement for chemical disinfectants that produce toxic disinfection byproducts. SWNT surface coatings are reported to reduce biofilm formation and metallic SWNTs, which induce significant membrane and oxidative stress, has great potential for this purpose. Metallic SWNT antibiofilm coatings have broad applications in numerous fields, including the medical and environmental sectors.

MATERIALS AND METHODS

Purification and Characterization of Single-Walled Carbon Nanotubes. The electronically metallic (>95% M), semiconducting (>95% M), and mixed (~30% M) single-walled carbon nanotubes (NanoIntegris, Skokie, IL) were separated by ultracentrifugation. The visible−near-IR absorption spectra of the surfactant-dispersed SWNTs were completed on an Agilent 8453 UV−vis spectrophotometer to evaluate their electronic nature. The surfactants (1% SDS and/or sodium cholate) were removed from the SWNTs by diluting the SWNT−surfactant solution with an equal volume of methanol. After 2 h, the SWNTs precipitated. The SWNTs were vacuum filtered using a 5-μm PVDF membrane (Millipore) and washed with copious amounts of distilled water. The filtered SWNTs were then placed into a concentrated HCl solution and bath sonicated for 1 h to dissolve any remaining metal catalyst. The SWNTs were then filtered and washed with copious amounts of water until the filtrate was at neutral pH. The acid-washed and filtered SWNTs were then subject to heating at 350 °C for 6 h. The prepared SWNTs were then dispersed by bath sonication in an appropriate solvent for the individual characterization and toxicity tests.

Transmission electron microscopy (Philips Tecnai F20 TEM) was used to examine the tubes for purity and defects. TEM image analysis (ImageJ, NIH) was used to determine SWNT diameters and lengths. The nanotube diameter and lengths were the average of at least 50 measurements. Raman spectra (Jasco NRS-1300) were recorded at an excitation wavelength of 785 nm. The SWNT Raman radial breathing mode was used to calculate average tube diameters,[46] and the D- and G-bands were integrated as a measure of tube defects and impurities. Thermogravimetric analysis (SETSYS 16/18) was performed from 200 to 1000 °C at a heating rate of 10 °C/min to determine the purity of the SWNTs. The concentration of aqueous SWNT solutions was quantified by measuring the dry weight of 100 μL aliquots with a microbalance (Mettler Toledo XS3DU). Details of the SWNT characterization procedures and data analysis methodologies are in the Supporting Information.

SWNT-Coated Filter. SWNTs were ultrasonically dispersed in DMSO at a concentration of 0.1−0.2 mg/mL. The SWNT suspension was then filtered through a 5 μm Omnipore PTFE membrane (Millipore) to form a SWNT-coating filter (35 mm in diameter) on top of the membrane. One hundred milliliters of ethanol were then filtered through the CNT-coated filter to remove residual DMSO, followed by filtering of 200 mL of deionized water to remove residual ethanol.

Cell Preparation. The bacterial strain (*E. coli* K12) was grown in LB medium at 37 °C and harvested at midexponential growth phase. Cells were washed twice and resuspended in a saline solution (0.9% NaCl) to remove residual macromolecules and other growth medium constituents.

Viability Assay. After the incubation in SWNT suspension (1 h) or on the SWNT-coated filter (0−75 min), the cells were stained with propidium iodide (PI; excitation/emission at 535 nm/617 nm; Molecular Probes, Invitrogen) for 15 min, and then counterstained with 4′,6-diamidino-2-phenylindole (DAPI, excitation/emission at 358 nm/461 nm; Sigma-Aldrich) for 5 min in the dark. In both cases, fluorescence images were taken under an epifluorescence microscope (Olympus BX40) with a U filter (364 nm/440 nm) for detecting cells stained with both PI and DAPI, and with an IB filter (464 nm/604 nm) for detecting cells stained with PI. Ten representative images were taken at 10× magnification at various locations for each specimen. Dead cells and the total number of cells were determined by direct cell counting on the CNT-coated filter, and 200−300 cells per image were counted. The percent of dead cells was determined from the ratio of the number of cells stained with PI divided by the number of cells stained with DAPI plus PI.

SEM of SWNT Inactivated Bacteria. Samples were filtered through a 0.22-μm PVDF membrane (Millipore) and fixed with 2.5% glutaraldehyde and 1% osmium tetraoxide. The cells were sputter-coated with gold (30 s, 30 mA) and then viewed under an XL30 scanning electron microscope (FEI, USA)

Thiol Oxidation and Quantification. The SWNT-mediated oxidation of glutathione (GSH) was completed under the following conditions: 0.4 mM GSH was made in a 50-mM bicarbonate buffer (pH 8.6) at a total volume of 250 μL in microcentrifuge tubes, and the reaction was initiated by spiking to 50 μg/mL of the various SWNTs. The tubes were then placed on a rotator (VWR Rotisserie Assembly) at room temperature (~22−23 °C) and covered with foil to prevent any photochemical reactions. Thiol concentration was quantified following Ellman's assay. Ellman's reagent, or 5,5′-dithio-*bis*-(2-nitrobenzoic acid) (DTNB, Invitrogen), reacts quantitatively with aqueous thiols to yield a yellow product that is analyzed colormetrically. Specifically, a 90-μL aliquot of the reaction solution was mixed with 157 μL of Tris-HCl (pH 8.3) and 3 μL of 100 mM DTNB. The assayed aliquots were then filtered through a 0.45-μm polyethersulfone filter (Whatman) to remove SWNTs to eliminate any background SWNT absorbance and/or scattering. The filtered 250 μL aliquot was then placed in a 96-well plate (BD Falcon 35-3915), and its absorbance at 412 nm was measured by a UV−vis spectrophotometer (SPECTRA max 340PC). The concentration of thiol was calculated using the absorbance at 412 nm, a path length of 1 cm, and a molar extinction coefficient of $\varepsilon = 14\,150\ M^{-1}\ cm^{-1}$. GSH oxidation by H_2O_2 (1 mM and 10 mM) was used as a positive control. After 1 h of reaction time, >99% of the GSH had been oxidized, in agreement with previously reported oxidation kinetics.[38]

Acknowledgment. C.D.V. acknowledges the Yale Institute of Biospheric Studies postdoctoral fellowship, K.R.Z. acknowledges the National Science Foundation Graduate Research Fellowship, and all acknowledge the Support of the National Science Foundation under Research Grant CBET- 0828795. The authors also thank Codruta Zoican Loebick for taking the TEM images.

Supporting Information Available: Details of the purification and analysis of the physicochemical properties of the single-walled carbon nanotubes used in this article. This material is available free of charge *via* the Internet at http://pubs.acs.org.

REFERENCES AND NOTES

1. Kroto, H. W.; Heath, J. R.; O'Brien, S. C.; Curl, R. F.; Smalley, R. E. C-60—Buckminsterfullerene. *Nature* **1985**, *318*, 162–163.
2. Iijima, S. Helical Microtubules of Graphitic Carbon. *Nature* **1991**, *354*, 56–58.
3. Thess, A.; Lee, R.; Nikolaev, P.; Dai, H. J.; Petit, P.; Robert, J.; Xu, C. H.; Lee, Y. H.; Kim, S. G.; Rinzler, A. G.; *et al.* Crystalline Ropes of Metallic Carbon Nanotubes. *Science* **1996**, *273*, 483–487.
4. Baughman, R. H.; Zakhidov, A. A.; de Heer, W. A. Carbon Nanotubes—The Route toward Applications. *Science* **2002**, *297*, 787–792.
5. Isaacs, J. A.; Tanwani, A.; Healy, M. L.; Dahlben, L. J. Economic Assessment of Single-Walled Carbon Nanotube Processes. *J. Nanopart. Res.* **2010**, *12*, 551–562.
6. Thayer, A. M. Carbon Nanotubes by the Metric Ton. *Chem. Eng. News* **2007**, *85*, 29–30.
7. Mauter, M. S.; Elimelech, M. Environmental Applications of Carbon-Based Nanomaterials. *Environ. Sci. Technol.* **2008**, *42*, 5843–5859.
8. Helland, A.; Wick, P.; Koehler, A.; Schmid, K.; Som, C. Reviewing the Environmental and Human Health Knowledge Base of Carbon Nanotubes. *Environ. Health Perspect.* **2007**, *115*, 1125–1131.
9. Kang, S.; Mauter, M. S.; Elimelech, M. Microbial Cytotoxicity of Carbon-Based Nanomaterials: Implications for River Water and Wastewater Effluent. *Environ. Sci. Technol.* **2009**, *43*, 2648–2653.
10. Lyon, D. Y.; Alvarez, P. J. J. Fullerene Water Suspension (nC(60)) Exerts Antibacterial Effects *via* ROS-Independent Protein Oxidation. *Environ. Sci. Technol.* **2008**, *42*, 8127–8132.
11. Fang, J. S.; Lyon, D. Y.; Wiesner, M. R.; Dong, J. P.; Alvarez, P. J. J. Effect of a Fullerene Water Suspension on Bacterial Phospholipids and Membrane Phase Behavior. *Environ. Sci. Technol.* **2007**, *41*, 2636–2642.
12. Kang, S.; Pinault, M.; Pfefferle, L. D.; Elimelech, M. Single-Walled Carbon Nanotubes Exhibit Strong Antimicrobial Activity. *Langmuir* **2007**, *23*, 8670–8673.
13. Liu, S. B.; Wei, L.; Hao, L.; Fang, N.; Chang, M. W.; Xu, R.; Yang, Y. H.; Chen, Y. Sharper and Faster "Nano Darts" Kill More Bacteria: A Study of Antibacterial Activity of Individually Dispersed Pristine Single-Walled Carbon Nanotube. *ACS Nano* **2009**, *3*, 3891–3902.
14. Arias, L. R.; Yang, L. J. Inactivation of Bacterial Pathogens by Carbon Nanotubes in Suspensions. *Langmuir* **2009**, *25*, 3003–3012.
15. Obraztsova, E. A.; Lukashev, E. P.; Zarubina, A. P.; Parkhomenko, I. M.; Yaminsky, I. V. Bactericidal Action of Single-Walled Carbon Nanotubes. *Phys. Bull. (Moscow University)* **2009**, *64*, 320–323.
16. Rodrigues, D. F.; Elimelech, M. Toxic Effects of Single-Walled Carbon Nanotubes in the Development of *E. coli* Biofilm. *Environ. Sci. Technol.* **2010**, *44*, 4583–4589.
17. Kang, S.; Herzberg, M.; Rodrigues, D. F.; Elimelech, M. Antibacterial Effects of Carbon Nanotubes: Size Does Matter. *Langmuir* **2008**, *24*, 6409–6413.
18. Oberdorster, E. Manufactured Nanomaterials (Fullerenes, C-60) Induce Oxidative Stress in the Brain of Juvenile Largemouth Bass. *Environ. Health Perspect.* **2004**, *112*, 1058–1062.

19. Sayes, C. M.; Fortner, J. D.; Guo, W.; Lyon, D.; Boyd, A. M.; Ausman, K. D.; Tao, Y. J.; Sitharaman, B.; Wilson, L. J.; Hughes, J. B.; *et al.* The Differential Cytotoxicity of Water-Soluble Fullerenes. *Nano Lett.* **2004**, *4*, 1881–1887.
20. Lyon, D. Y.; Brunet, L.; Hinkal, G. W.; Wiesner, M. R.; Alvarez, P. J. J. Antibacterial Activity of Fullerene Water Suspensions (nC(60)) Is Not Due to ROS-Mediated Damage. *Nano Lett.* **2008**, *8*, 1539–1543.
21. Kang, S.; Mauter, M. S.; Elimelech, M. Physicochemical Determinants of Multiwalled Carbon Nanotube Bacterial Cytotoxicity. *Environ. Sci. Technol.* **2008**, *42*, 7528–7534.
22. Hamada, N.; Sawada, S.; Oshiyama, A. New One-Dimensional Conductors—Graphitic Microtubules. *Phys. Rev. Lett.* **1992**, *68*, 1579–1581.
23. Saito, R.; Fujita, M.; Dresselhaus, G.; Dresselhaus, M. S. Electronic-Structure of Chiral Graphene Tubules. *Appl. Phys. Lett.* **1992**, *60*, 2204–2206.
24. Li, N.; Wang, X. M.; Ren, F.; Haller, G. L.; Pfefferle, L. D. Diameter Tuning of Single-Walled Carbon Nanotubes with Reaction Temperature Using a Co Monometallic Catalyst. *J. Phys. Chem. C* **2009**, *113*, 10070–10078.
25. Li, Y. M.; Kim, W.; Zhang, Y. G.; Rolandi, M.; Wang, D. W.; Dai, H. J. Growth of Single-Walled Carbon Nanotubes from Discrete Catalytic Nanoparticles of Various Sizes. *J. Phys. Chem. B* **2001**, *105*, 11424–11431.
26. Arnold, M. S.; Green, A. A.; Hulvat, J. F.; Stupp, S. I.; Hersam, M. C. Sorting Carbon Nanotubes by Electronic Structure Using Density Differentiation. *Nat. Nanotechnol.* **2006**, *1*, 60–65.
27. Strano, M. S.; Dyke, C. A.; Usrey, M. L.; Barone, P. W.; Allen, M. J.; Shan, H. W.; Kittrell, C.; Hauge, R. H.; Tour, J. M.; Smalley, R. E. Electronic Structure Control of Single-Walled Carbon Nanotube Functionalization. *Science* **2003**, *301*, 1519–1522.
28. Banerjee, S.; Wong, S. S. Selective Metallic Tube Reactivity in the Solution-Phase Osmylation of Single-Walled Carbon Nanotubes. *J. Am. Chem. Soc.* **2004**, *126*, 2073–2081.
29. Yang, C. M.; Park, J. S.; An, K. H.; Lim, S. C.; Seo, K.; Kim, B.; Park, K. A.; Han, S.; Park, C. Y.; Lee, Y. H. Selective Removal of Metallic Single-Walled Carbon Nanotubes with Small Diameters by Using Nitric and Sulfuric Acids. *J. Phys. Chem. B* **2005**, *109*, 19242–19248.
30. Zhang, G. Y.; Qi, P. F.; Wang, X. R.; Lu, Y. R.; Li, X. L.; Tu, R.; Bangsaruntip, S.; Mann, D.; Zhang, L.; Dai, H. J. Selective Etching of Metallic Carbon Nanotubes by Gas-Phase Reaction. *Science* **2006**, *314*, 974–977.
31. Kanungo, M.; Lu, H.; Malliaras, G. G.; Blanchet, G. B. Suppression of Metallic Conductivity of Single-Walled Carbon Nanotubes by Cycloaddition Reactions. *Science* **2009**, *323*, 234–237.
32. Lian, Y. F.; Maeda, Y.; Wakahara, T.; Akasaka, T.; Kazaoui, S.; Minami, N.; Choi, N.; Tokumoto, H. Assignment of the Fine Structure in the Optical Absorption Spectra of Soluble Single-Walled Carbon Nanotubes. *J. Phys. Chem. B* **2003**, *107*, 12082–12087.
33. Kim, U. J.; Furtado, C. A.; Liu, X. M.; Chen, G. G.; Eklund, P. C. Raman and IR Spectroscopy of Chemically Processed Single-Walled Carbon Nanotubes. *J. Am. Chem. Soc.* **2005**, *127*, 15437–15445.
34. Kongkanand, A.; Dominguez, R. M.; Kamat, P. V. Single Wall Carbon Nanotube Scaffolds for Photoelectrochemical Solar Cells. Capture and Transport of Photogenerated Electrons. *Nano Lett.* **2007**, *7*, 676–680.
35. Kongkanand, A.; Kamat, P. V. Electron Storage in Single Wall Carbon Nanotubes. Fermi Level Equilibration in Semiconductor−SWCNT Suspensions. *ACS Nano* **2007**, *1*, 13–21.
36. Fahey, R. C.; Brown, W. C.; Adams, W. B.; Worsham, M. B. Occurrence of Glutathione in Bacteria. *J. Bacteriol.* **1978**, *133*, 1126–1129.
37. Schafer, F. Q.; Buettner, G. R. Redox Environment of the Cell as Viewed through the Redox State of the Glutathione Disulfide/Glutathione Couple. *Free Radical Biol. Med.* **2001**, *30*, 1191–1212.
38. Winterbourn, C. C.; Metodiewa, D. Reactivity of Biologically Important Thiol Compounds with Superoxide and Hydrogen Peroxide. *Free Radical Biol. Med.* **1999**, *27*, 322–328.
39. Carmel-Harel, O.; Storz, G. Roles of the Glutathione- and Thioredoxin-Dependent Reduction Systems in the *Escherichia coli* and *Saccharomyces cerevisiae* Responses to Oxidative Stress. *Annu. Rev. Microbiol.* **2000**, *54*, 439–461.
40. Ellman, G. L. Tissue Sulfhydryl Groups. *Arch. Biochem. Biophys.* **1959**, *82*, 70–77.
41. Kemper, J. M.; Ammar, E.; Mitch, W. A. Abiotic Degradation of Hexahydro-1,3,5-trinitro-1,3,5-triazine in the Presence of Hydrogen Sulfide and Black Carbon. *Environ. Sci. Technol.* **2008**, *42*, 2118–2123.
42. Dunnivant, F. M.; Schwarzenbach, R. P.; Macalady, D. L. Reduction of Substituted Nitrobenzenes in Aqueous Solutions Containing Natural Organic Matter. *Environ. Sci. Technol.* **1992**, *26*, 2133–2141.
43. Lipnick, R. L. Structure−Activity Relationships. In *Fundamentals of Aquatic Toxicology*, 2nd ed.; Rand, G. M., Ed.; Taylor and Francis Publishers: Washington, DC, 1995; pp 609−655.
44. Verhaar, H. J. M.; Vanleeuwen, C. J.; Hermens, J. L. M. Classifying Environmental-Pollutants. 1. Structure−Activity-Relationships for Prediction of Aquatic Toxicity. *Chemosphere* **1992**, *25*, 471–491.
45. Escher, B. I.; Bramaz, N.; Eggen, R. I. L.; Richter, M. *In Vitro* Assessment of Modes of Toxic Action of Pharmaceuticals in Aquatic Life. *Environ. Sci. Technol.* **2005**, *39*, 3090–3100.
46. Dresselhaus, M. S.; Dresselhaus, G.; Saito, R.; Jorio, A. Raman Spectroscopy of Carbon Nanotubes. *Phys. Rep.* **2005**, *409*, 47–99.